RECONSTRUCTION OF AN ELLIPTICAL INCLUSION IN THE INVERSE CONDUCTIVITY PROBLEM

ANDREAS KARAGEORGHIS AND DANIEL LESNIC

Abstract. This study reports on a numerical investigation into the open problem of the unique reconstruction of an elliptical inclusion in the potential field from a single set of nontrivial Cauchy data. The investigation is based on approximating the potential fields of a composite material as a linear combination of fundamental solutions for the Laplace equation with sources shifted outside the solution domain and its boundary. The coefficients of these finite linear combinations are unknown along with the centre, the lengths of the semi-axes and the orientation of the sought ellipse. These are determined by minimizing the least-squares objective functional describing the gap between the given and computed data. The extension of the proposed technique for the reconstruction of two ellipses is also considered.

1. Introduction

One hundred years ago Johann Radon discovered the transform on which the principles of X-ray tomography are based. However, it took fifty years for its importance to be realized and acknowledged. The mathematical foundation of tomographic scanning was produced by A. Calderon in his seminal presentation in 1980. Since then, numerous breakthroughs have occurred on establishing the uniqueness of recovering the heterogeneous conductivity of a medium from the Dirichlet-to-Neumann boundary map culminating with the proof in two dimensions [2] for the unique recovery of L^∞-conductivities. However, one of the drawbacks of the Calderon formulation is that infinitely dimensional input data are required. Therefore, in order to render the formulation more practical, a series of papers was initiated by V. Isakov in the late eighties concerning the recovery of a piecewise conductivity from a finite set of Cauchy data [7, 8]. This latter problem may be reformulated as a transmission problem for determining the interface between materials having different conductivities.

Convex or concave polygonal interfaces are uniquely identifiable from one or two sets of Cauchy data [4, 26] but smooth surfaces are more difficult to investigate and, up to now, uniqueness with one set of Cauchy data is only known for circular or spherical interfaces [12, 14]; also confirmed by stability estimates [16, 27] and successful numerical reconstructions [15, 21]. However, for other smooth shapes, e.g. ellipses, identification with one measurement is only known for perfectly conductive or insulated interfaces, i.e. piecewise extreme conductivities of ∞ or 0, [13]. Therefore,

Date: April 9, 2018.

2010 *Mathematics Subject Classification.* Primary 65N35; Secondary 65N21, 65N38.

Key words and phrases. Elliptical inclusion, inverse conductivity problem, method of fundamental solutions.

encouraged by some successful numerical investigations in which arbitrary smooth inclusions were recovered using either the boundary element method (BEM) [5, 6] or the method of fundamental solutions (MFS) [17], see also [18, 19], it is the purpose of this study to investigate the numerical identification of an elliptical interface from one measurement of Cauchy data in order to offer insight into the uniqueness of the yet unsolved inverse elliptical conductivity problem [9]. We note that the shape of an ellipse for an interface is typical for both damage and porosity geometries [3].

The paper is organized as follows. In Section 2 we provide the mathematical formulation of the inverse conductivity problem for identifying an elliptical inclusion from one Cauchy boundary data measurement. The approximation of the resulting transmission problem in a composite material using the MFS is presented in Section 3 and the resulting nonlinear minimization problem is described in Section 4. Several examples concerning the reconstruction of circular, elliptical and bi-elliptical inclusions are presented and discussed in Sections 5 and 6. Finally, in Section 7 we present some conclusions and ideas for future work.

2. Mathematical formulation

We consider the inverse conductivity problem of determining a piecewise constant isotropic conductivity $1+(\kappa-1)\mathcal{X}(D)$, where D is an unknown inclusion (in this paper an ellipse or a collection of ellipses) compactly contained in a given planar bounded domain $\Omega \subset \mathbb{R}^2$, where $\mathcal{X}(D)$ is the characteristic function of the domain D and $\kappa \neq 1$ is a given positive constant, from a single measurement of the current flux induced by a boundary potential prescribed on $\partial\Omega$ or vice versa. This inverse problem represents the mathematical formulation of the continuous model of electrical capacitance/impedance tomography. It can be recast as the following transmission problem governed by the Laplace equations:

$$\Delta u_1 = 0 \quad \text{in} \quad \Omega \backslash \overline{D}, \tag{2.1a}$$

$$\Delta u_2 = 0 \quad \text{in} \quad D, \tag{2.1b}$$

subject to the boundary conditions

$$u_1 = f \not\equiv \text{constant} \quad \text{on} \quad \partial\Omega, \tag{2.1c}$$

$$\frac{\partial u_1}{\partial n} = g \quad \text{on} \quad \partial\Omega, \tag{2.1d}$$

and the transmission perfect contact conditions

$$u_1 = u_2 \quad \text{on} \quad \partial D, \tag{2.1e}$$

$$\frac{\partial u_1}{\partial n^-} = -\kappa \frac{\partial u_2}{\partial n^+} \quad \text{on} \quad \partial D, \tag{2.1f}$$

where $\Omega \subset \mathbb{R}^2$ is a bounded simply-connected planar domain with smooth boundary $\partial\Omega$ and ∂D is the ellipse defined by

$$x = X + r(\vartheta)\cos\vartheta, \quad y = Y + r(\vartheta)\sin\vartheta, \quad \vartheta \in [0, 2\pi), \tag{2.1g}$$

and

$$r(\vartheta) = \frac{1}{\sqrt{\dfrac{\cos^2(\vartheta - \varphi)}{a^2} + \dfrac{\sin^2(\vartheta - \varphi)}{b^2}}}. \tag{2.1h}$$

In (2.1g), (X, Y) is the centre of the ellipse, $2a$ and $2b$ are the lengths of the major and minor axes of the ellipse, respectively, and φ is the angle the major axis makes with the horizontal. Similar considerations can be made for an ellipsoid in three dimensions using spherical coordinates.

3. The method of fundamental solutions (MFS)

The MFS for the Laplace equation in a bounded domain may be viewed as a numerical discretization of a single-layer potential boundary integral representation in which the given boundary values and the sought solution are defined on different curves [11]. Consequently, a solution to the Laplace equation (2.1a) is given as a linear combination of fundamental solutions of the form

$$u_1(\boldsymbol{c}, \boldsymbol{\xi}; \boldsymbol{x}) = \sum_{k=1}^{M+N} c_k \, G(\boldsymbol{x}, \boldsymbol{\xi}_k), \quad \boldsymbol{x} \in \overline{\Omega} \backslash D, \tag{3.1}$$

where G is the fundamental solution of the two-dimensional Laplace equation, given by

$$G(\boldsymbol{\xi}, \boldsymbol{x}) = -\frac{1}{2\pi} \log \mid \boldsymbol{\xi} - \boldsymbol{x} \mid. \tag{3.2}$$

The sources $(\boldsymbol{\xi}_k)_{k=\overline{1,M}}$ are located outside $\overline{\Omega}$, while the sources $(\boldsymbol{\xi}_k)_{k=\overline{M+1,M+N}}$ are located in D. The geometry of the problem and the location of the source points are sketched in Figure 1. More specifically, the sources $(\boldsymbol{\xi}_k)_{k=\overline{1,M}}$ are located on a (moving) pseudo-boundary $\partial\Omega'$ similar to (dilation $\delta_1 > 0$) $\partial\Omega$ while the sources $(\boldsymbol{\xi}_k)_{k=\overline{M+1,M+N}}$ are located on a (moving) pseudo-boundary ∂D^- similar to (contraction $\delta_2 > 0$) ∂D.

Similarly, we seek an approximation to the solution of the Laplace equation (2.1b) in the form

$$u_2(\boldsymbol{d}, \boldsymbol{\eta}; \boldsymbol{x}) = \sum_{k=1}^{N} d_k \, G(\boldsymbol{x}, \boldsymbol{\eta}_k), \quad \boldsymbol{x} \in \overline{D}, \tag{3.3}$$

where the sources $(\boldsymbol{\eta}_k)_{k=\overline{1,N}}$ are located outside $\overline{D}$ on a (moving) pseudo-boundary ∂D^+ similar to (dilation $\delta_3 > 0$) ∂D. The idea of using a fictitious moving pseudo-boundary in inverse geometric problems was first proposed in [19].

Since we have $2M$ Cauchy boundary conditions (2.1c) - (2.1d) and $2N$ interface conditions (2.1e) - (2.1f) we have a total of $2M + 2N$ equations. The unknowns consist of the $M + N$ coefficients $(c_k)_{k=\overline{1,M+N}}$, the N coefficients $(d_k)_{k=\overline{1,N}}$, the centre (X, Y), the semi-axes of the ellipse a and b, the angle φ and the three dilation/contraction coefficients $\delta_1, \delta_2, \delta_3$, yielding a total of $M + 2N + 8$ unknowns. In order to avoid an under-determined situation we require $M \geq 8$.

We next define the collocation points $(\boldsymbol{x}_\ell)_{\ell=\overline{1,M+N}}$, where $\boldsymbol{x}_\ell = (x_\ell, y_\ell)$, the sources $(\boldsymbol{\xi}_k)_{k=\overline{1,M+N}}$, where $\boldsymbol{\xi}_k = (\xi_k^x, \xi_k^y)$, and the sources $(\boldsymbol{\eta}_k)_{k=\overline{1,N}}$, where $\boldsymbol{\eta}_k = (\eta_k^x, \eta_k^y)$. Without loss of generality,

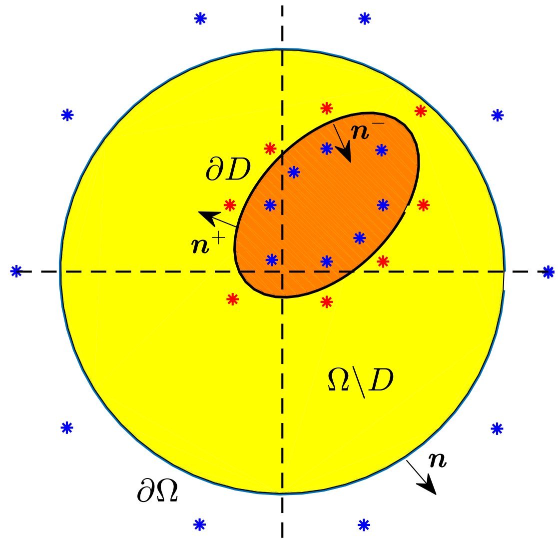

FIGURE 1. Geometry of the problem. The asterisks ($*$) denote the source points located on fictitious pseudo-boundaries $\partial\Omega'$ (dilation of $\partial\Omega$), ∂D^- (contraction of ∂D) and ∂D^+ (dilation of ∂D).

we shall assume that the (known) fixed exterior boundary $\partial\Omega$ is a circle of radius R. As a result, the outer boundary collocation and source points are chosen as

$$\boldsymbol{x}_m = R\left(\cos\theta_m, \sin\theta_m\right), \quad m=\overline{1,M}, \tag{3.4}$$
$$\boldsymbol{\xi}_m = \delta_1 R\left(\cos\theta_m, \sin\theta_m\right), \quad m=\overline{1,M}, \tag{3.5}$$

respectively, where $\theta_m = \frac{2\pi(m-1)}{M}$, $m=\overline{1,M}$, and the (unknown) parameter $\delta_1 \in (1, S_1)$ with $S_1 > 1$ prescribed.
We choose the inner boundary collocation and source points as

$$x_{M+n} = X + r(\vartheta_n)\cos\vartheta_n,\ y_{M+n} = Y + r(\vartheta_n)\sin\vartheta_n, \tag{3.6}$$

$$\xi^x_{M+n} = X + \delta_2\, r(\vartheta_n)\cos\vartheta_n,\ \xi^y_{M+n} = Y + \delta_2\, r(\vartheta_n)\sin\vartheta_n, \tag{3.7}$$

and

$$\eta^x_n = X + \delta_3\, r(\vartheta_n)\cos\vartheta_n,\ \eta^y_n = Y + \delta_3\, r(\vartheta_n)\sin\vartheta_n, \tag{3.8}$$

$n=\overline{1,N}$ where $\vartheta_n = \frac{2\pi(n-1)}{N}$, $n=\overline{1,N}$, and the (unknown) parameter $\delta_2 \in (S_2, 1)$ (with $0<S_2<1$ prescribed) and the (unknown) parameter $\delta_3 \in (1, S_3)$ with $S_3 > 1$ prescribed.

4. Implementational details

The coefficients $(c_k)_{k=\overline{1,M+N}}$ in (3.1), the coefficients $(d_k)_{k=\overline{1,N}}$ in (3.3), the contraction coefficient δ_2 and the dilation coefficients δ_1, δ_3 in (3.5), (3.7), (3.8), the coordinates of the centre (X, Y), the half-lengths of the major and minor axes a and b in (2.1g) and the angle φ in (2.1g) can be determined by imposing the boundary conditions (2.1c)-(2.1d) and the transmission conditions (2.1e)-(2.1f) in a least-squares sense. This leads to the minimization of the functional

$$S(\boldsymbol{c}, \boldsymbol{d}, \boldsymbol{\delta}, \boldsymbol{C}, a, b, \varphi) := \sum_{j=1}^{M} \left[u_1(\boldsymbol{c}, \boldsymbol{\xi}; \boldsymbol{x}_j) - f(\boldsymbol{x}_j)\right]^2 + \sum_{j=1}^{M} \left[\frac{\partial u_1}{\partial n}(\boldsymbol{c}, \boldsymbol{\xi}; \boldsymbol{x}_j) - g(\boldsymbol{x}_j)\right]^2$$

$$+ \sum_{j=1}^{N} \left[u_1(\boldsymbol{c}, \boldsymbol{\xi}; \boldsymbol{x}_{M+j}) - u_2(\boldsymbol{d}, \boldsymbol{\eta}; \boldsymbol{x}_{M+j})\right]^2 + \sum_{j=1}^{N} \left[\frac{\partial u_1}{\partial n^-}(\boldsymbol{c}, \boldsymbol{\xi}; \boldsymbol{x}_{M+j}) + \kappa \, \frac{\partial u_2}{\partial n^+}(\boldsymbol{d}, \boldsymbol{\eta}; \boldsymbol{x}_{M+j})\right]^2, \quad (4.1)$$

where $\boldsymbol{c} = (c_1, c_2, \ldots, c_{M+N})$, $\boldsymbol{d} = (d_1, d_2, \ldots, d_N)$, $\boldsymbol{\delta} = (\delta_1, \delta_2, \delta_3)$ and $\boldsymbol{C} = (X, Y)$.

Remarks.

(i) In (4.1), the outward normal vector $\boldsymbol{n}$ is defined as follows:

$$\boldsymbol{n} = \cos\vartheta \, \boldsymbol{i} + \sin\vartheta \, \boldsymbol{j}\,, \quad \text{if} \quad \boldsymbol{x} \in \partial\Omega, \quad (4.2)$$

$$\boldsymbol{n}^{\pm} = \pm \frac{1}{\sqrt{r^2(\vartheta) + r'^2(\vartheta)}} \Big(r'(\vartheta)\sin\vartheta + r(\vartheta)\cos\vartheta, \; r(\vartheta)\sin\vartheta - r'(\vartheta)\cos\vartheta\Big), \quad \text{if} \quad \boldsymbol{x} \in \partial D, \quad (4.3)$$

where $\boldsymbol{i} = (1, 0)$ and $\boldsymbol{j} = (0, 1)$. Moreover, r is given by (2.1g) and

$$r'(\vartheta) = \frac{1}{2}\left(\frac{1}{a^2} - \frac{1}{b^2}\right) \frac{\sin\left(2(\vartheta - \varphi)\right)}{\left(\sqrt{\dfrac{\cos^2(\vartheta - \varphi)}{a^2} + \dfrac{\sin^2(\vartheta - \varphi)}{b^2}}\right)^3}\,. \quad (4.4)$$

(ii) The minimization of functional (4.1) is carried out using the MATLAB© [22] optimization toolbox routine `lsqnonlin` which solves nonlinear least squares problems. The routine `lsqnonlin` does not require the user to provide the gradient and, in addition, it offers the option of imposing lower and upper bounds on the elements of the vector of unknowns $\boldsymbol{x} = (\boldsymbol{c}, \boldsymbol{d}, \boldsymbol{\delta}, \boldsymbol{C}, a, b, \varphi)$ through the vectors `lb` and `up`. Such geometrical constraints include $a \in (0, R), b \in (0, R), \varphi \in [0, \pi], X \in (-R, R)$ and $Y \in (-R, R)$.

(iii) Since the ellipse D is parametrised by a small number (five) of parameters there is no need to regularize the least squares functional (4.1) in order to obtain a stable solution.

5. Numerical examples

In all the figures presented in this section, the exact elliptic inclusion is plotted using a red dash-dot line ($- \cdot -$), while the numerically retrieved inclusion is plotted using a blue dashed line ($---$). We also take $R = 1$, i.e. Ω is the unit disk and chose $\kappa = 10$ in (2.1f). Also, we chose $S_1 = S_3 = 2, S_2 = 0.1$. We run the MFS inverse problem solver with $M = 48$ and $N = 96$. The value of M is not so important but N should be sufficiently large to ensure that (3.6) represents a "smooth" ellipse. We note that when D and κ are both unknown, uniqueness still holds with one set of Cauchy data (2.1c)-(2.1d) of a special type (roughly speaking, the Dirichlet data f in (2.1c) has only one maximum on $\partial\Omega$), D is searched in the class of convex polygons and κ is an unknown constant in the intervals $(0, \infty) \setminus \{1\}$, as proved in Theorem 5.1 of [1]; however the numerically accurate and stable recovery of κ is difficult [21, 5].

5.1. **Example 1.** We first tested the method by considering an example for which an exact solution is known and given by, [17, 21],

$$u_1(x,y) = x - \frac{(1-\kappa)x}{2}\left[1 - \frac{r_0^2}{x^2+y^2}\right], \quad (x,y) \in \Omega\backslash D, \tag{5.1}$$

$$u_2(x,y) = x, \quad (x,y) \in D, \tag{5.2}$$

$$D = B(\mathbf{0}; r_0) = \left\{(x,y) \in \mathbb{R}^2 : x^2 + y^2 < r_0^2\right\}, \tag{5.3}$$

where $r_0 \in (0,1)$ (recall that $\kappa = 10$) and $\Omega = B(\mathbf{0}, 1)$.
This exact solution satisfies problem (2.1) with

$$f(x,y) = x - \frac{(1-\kappa)(1-r_0^2)x}{2}, \quad (x,y) \in \partial\Omega, \tag{5.4}$$

and

$$g(x,y) = \frac{\left(1+\kappa+(\kappa-1)r_0^2\right)x}{2} \quad (x,y) \in \partial\Omega. \tag{5.5}$$

We took the Cauchy data (5.4) and (5.5) given for $r_0 = 0.3$, which constitutes the exact solution for the circular inclusion (5.3). Note that since we are using the analytical expression (5.5) for the Neumann data (2.1d) we also have some numerical noise included in the inverse problem which is solved numerically.

The initial guesses for $\boldsymbol{c}$, $\boldsymbol{d}$ and $\boldsymbol{\delta}$ are taken to be $\boldsymbol{c}_0 = \mathbf{0}$, $\boldsymbol{d}_0 = \mathbf{0}$, $\boldsymbol{\delta}_0 = (1.8, 0.8, 1.2)$, and we investigate two (different) arbitrary initial guesses for $\boldsymbol{C}, a, b$ and φ, namely,

$$\boldsymbol{C}_0 = (0.5, 0.3),\ a_0 = 0.4,\ b_0 = 0.2,\ \varphi_0 = \pi/3, \tag{5.6a}$$

and

$$\boldsymbol{C}_0 = (-0.5, 0.3),\ a_0 = 0.3,\ b_0 = 0.1,\ \varphi_0 = \pi/2. \tag{5.6b}$$

In Figure 2 we present the results obtained with various numbers of iterations `niter`, for both cases of initial guesses (5.6a) and (5.6b). As may be observed from this figure, the case with initial guess (5.6b) converges slower than the case with initial guess (5.6a). This is probably due to the thinner shape of the initial ellipse in (5.6b).

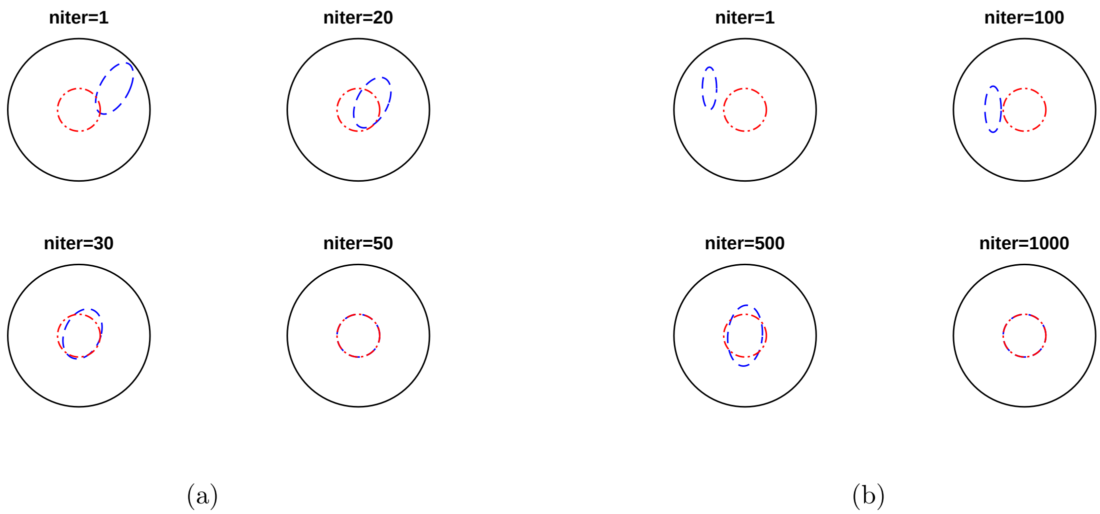

FIGURE 2. Example 1: Identifications of the circular inclusion (5.3) with $r_0 = 0.3$ for the initial guesses (5.6a) (in (a)) and (5.6b) (in (b)).

5.2. **Example 2.** The Dirichlet data (2.1c) on $\partial\Omega$ is taken as [10]

$$u(1, \vartheta) = f(\vartheta) = \mathrm{e}^{-\cos^2\vartheta}, \quad \vartheta \in [0, 2\pi). \tag{5.7}$$

Since in this case no analytical solution is available, the Neumann data (2.1d) is simulated by solving the direct well-posed problem (2.1a), (2.1b), (2.1c) and (2.1e)-(2.1f), using the MFS with $M = 200, N = 100$ and $\delta_1 = 2, \delta_2 = 0.9, \delta_3 = 1.1$. An inverse crime is avoided since the inverse solver is applied using $N = 96, M = 48$. This also generates some small numerical noise in the data (2.1d) which is inverted. The initial values of the unknowns are taken as $\boldsymbol{c}_0 = \mathbf{0}$, $\boldsymbol{d}_0 = \mathbf{0}$, $\boldsymbol{\delta}_0 = (1.6, 0.8, 1.2)$, $\boldsymbol{C}_0 = (0, 0)\,, a_0 = b_0 = 0.3$. We have also considered other initial guesses for $a_0 = b_0 = i/10$ for $i = 1, 2, \ldots, 8$, and convergent results to the exact target were obtained. However, the routine employed requires a good initial guess for the angle φ in order to ensure convergence. Such a good a priori initial guess can be provided either from the physics of the problem or by running a prior global optimization based on an evolutionary search technique such as the genetic algorithm [24] or the particle swarm algorithm [5].

We considered the following cases:

(a) Ellipse to be reconstructed: $\boldsymbol{C} = (-0.4, -0.1), a = 0.4, b = 0.2, \varphi = \pi/3$.
Initial guess for angle: $\varphi_0 = \pi/6$.
(b) Ellipse to be reconstructed: $\boldsymbol{C} = (-0.5, -0.2), a = 0.3, b = 0.1, \varphi = \pi/6$.
Initial guess for angle: $\varphi_0 = \pi/8$.
(c) Ellipse to be reconstructed: $\boldsymbol{C} = (0.3, 0.1), a = 0.4, b = 0.1, \varphi = \pi/4$.
Initial guess for angle: $\varphi_0 = \pi/5$.
(d) Ellipse to be reconstructed: $\boldsymbol{C} = (0.4, 0.2), a = 0.4, b = 0.1, \varphi = \pi/4$.
Initial guess for angle: $\varphi_0 = \pi/5$.

The convergence of the objective function (4.1), as a function of the number of iterations is presented in Figure 3, while the inclusion identifications at various iteration numbers, `niter`, for cases (a)-(d) are presented in Figures 4(a)-4(d). We observe that the thinner the ellipse the slower the convergence. Also, the greater the distance of the centre of the ellipse from the origin the slower the convergence (compare cases (c) and (d)).

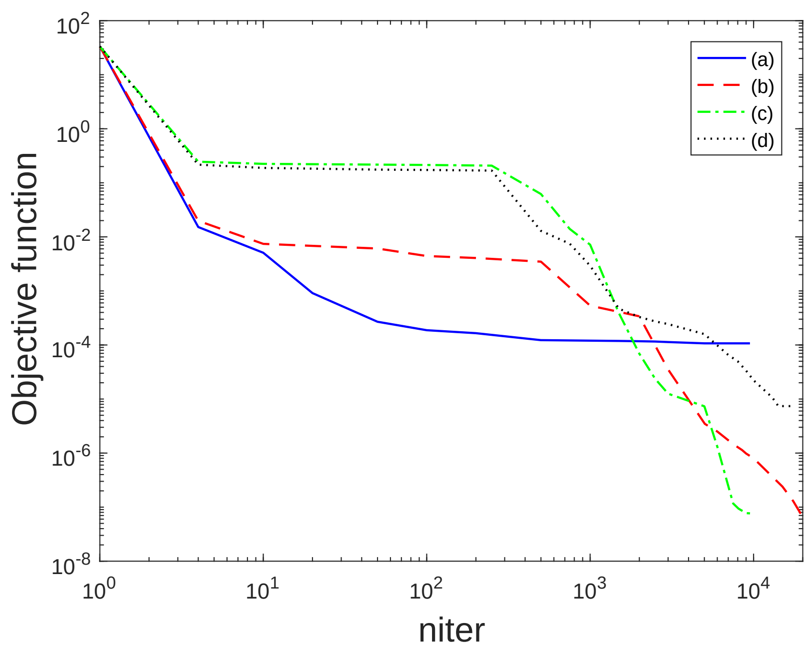

FIGURE 3. Example 2: The objective function (4.1), as a function of the number of iterations for cases (a)-(d). Note that in cases (a) and (c), the routine terminates prior to reaching the maximum number of iterations which was set to 20000.

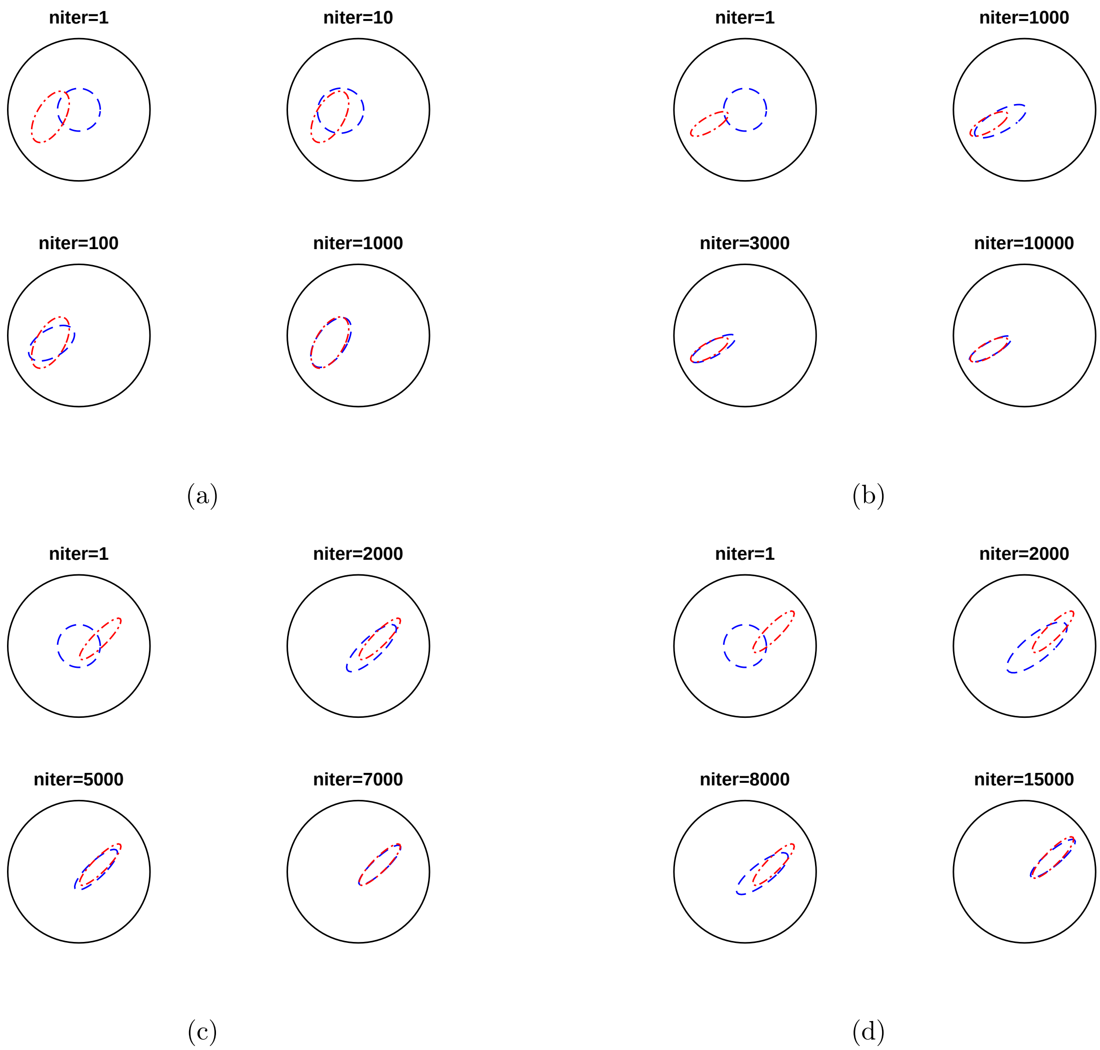

FIGURE 4. Example 2: Identifications of the elliptical inclusions (a)-(d) at various iteration numbers.

6. Extension to multiple inclusions

We now consider the following inverse boundary value problem with two inclusions:

$$\Delta u_1 = 0 \quad \text{in} \quad \Omega \backslash \left(\overline{D_1 \cup D_2}\right), \tag{6.1a}$$

$$\Delta u_2^{(1)} = 0 \quad \text{in} \quad D_1, \tag{6.1b}$$

$$\Delta u_2^{(2)} = 0 \quad \text{in} \quad D_2, \tag{6.1c}$$

subject to the Cauchy data

$$u_1 = f \not\equiv \text{constant} \quad \text{on} \quad \partial\Omega, \tag{6.1d}$$

$$\frac{\partial u_1}{\partial n} = g \quad \text{on} \quad \partial\Omega, \tag{6.1e}$$

and the transmission conditions

$$u_1 = u_2^{(1)} \quad \text{on} \quad \partial D_1, \tag{6.1f}$$

$$\frac{\partial u_1}{\partial n^-} = -\kappa_1 \frac{\partial u_2^{(1)}}{\partial n^+} \quad \text{on} \quad \partial D_1, \tag{6.1g}$$

$$u_1 = u_2^{(2)} \quad \text{on} \quad \partial D_2, \tag{6.1h}$$

$$\frac{\partial u_1}{\partial n^-} = -\kappa_2 \frac{\partial u_2^{(2)}}{\partial n^+} \quad \text{on} \quad \partial D_2, \tag{6.1i}$$

where $\Omega \subset \mathbb{R}^2$ is a bounded simply-connected planar domain with smooth boundary $\partial\Omega$ and ∂D_1, ∂D_2 are ellipses of conductivities $0 < \kappa_1, \kappa_2 \neq 1$ defined by

$$x = X_\ell + r_\ell(\vartheta)\cos\vartheta, \quad y = Y_\ell + r_\ell(\vartheta)\sin\vartheta, \quad \vartheta \in [0, 2\pi), \quad \ell = 1, 2, \tag{6.1j}$$

where

$$r_\ell(\vartheta) = \frac{1}{\sqrt{\dfrac{\cos^2(\vartheta - \varphi_\ell)}{a_\ell^2} + \dfrac{\sin^2(\vartheta - \varphi_\ell)}{b_\ell^2}}}, \quad \ell = 1, 2. \tag{6.1k}$$

In (6.1j) and (6.1k), (X_ℓ, Y_ℓ), $\ell = 1, 2$, are the centres of the ellipses, $2a_\ell$ and $2b_\ell$, $\ell = 1, 2$, are the lengths of the major and minor axes of the ellipses, respectively, and φ_ℓ, $\ell = 1, 2$, are the angles the major axes of the ellipses make with the horizontal. We assume that $\overline{D}_1$ and $\overline{D}_2 \subset \Omega$, and that $\overline{D}_1 \cap \overline{D}_2 = \emptyset$.

In the MFS, we first seek an approximation to the solution of the Laplace equation (6.1a) as a linear combination of fundamental solutions of the form

$$u_1(\boldsymbol{c}, \boldsymbol{\xi}; \boldsymbol{x}) = \sum_{k=1}^{M+N_1+N_2} c_k \, G(\boldsymbol{x}, \boldsymbol{\xi}_k), \quad \boldsymbol{x} \in \overline{\Omega} \backslash (D_1 \cup D_2). \tag{6.2}$$

The sources $(\boldsymbol{\xi}_k)_{k=\overline{1,M}}$ are located outside $\overline{\Omega}$, while the sources $(\boldsymbol{\xi}_k)_{k=\overline{M+1,M+N_1}}$ are located in D_1 and the sources $(\boldsymbol{\xi}_k)_{k=\overline{M+N_1+1,M+N_1+N_2}}$ are located in D_2. More specifically, as described in Section 3, the sources $(\boldsymbol{\xi}_k)_{k=\overline{1,M}}$ are located on a (moving) pseudo-boundary $\partial\Omega'$ similar to (dilation $\delta_1 > 0$) $\partial\Omega$. The sources $(\boldsymbol{\xi}_k)_{k=\overline{M+1,M+N_1}}$ are located on a (moving) pseudo-boundary ∂D_1^- similar to (contraction $\delta_2^{(1)} > 0$) ∂D_1, while the sources $(\boldsymbol{\xi}_k)_{k=\overline{M+N_1+1,M+N_1+N_2}}$ are located on a (moving) pseudo-boundary ∂D_2^- similar to (contraction $\delta_2^{(2)} > 0$) ∂D_2.

Similarly, we seek approximations to the solutions of the Laplace equation (6.1b)-(6.1c) in the form

$$u_2^{(\ell)}(\boldsymbol{d}^\ell, \boldsymbol{\eta}^\ell; \boldsymbol{x}) = \sum_{k=1}^{N_\ell} d_k^\ell \, G(\boldsymbol{x}, \boldsymbol{\eta}_k^\ell), \quad \boldsymbol{x} \in \overline{D}_\ell, \quad \ell = 1, 2, \tag{6.3}$$

where the sources $\left(\boldsymbol{\eta}_k^\ell\right)_{k=\overline{1,N_\ell}}$ are located outside $\overline{D}_\ell$ on a (moving) pseudo-boundary ∂D_ℓ^+ similar to (dilation $\delta_{(3)}^\ell > 1$) ∂D_ℓ, $\ell = 1, 2$.

Since we have $2M$ Cauchy boundary conditions (6.1d) - (6.1e) and $2(N_1 + N_2)$ interface conditions (6.1f) - (6.1i), we have a total of $2M + 2(N_1 + N_2)$ equations. The unknowns consist of the $M + N$ coefficients $(c_k)_{k=\overline{1,M+N_1+N_2}}$, the N_ℓ coefficients $\left(d_k^\ell\right)_{k=\overline{1,N_\ell}}$, $\ell = 1, 2$, the centres (X_ℓ, Y_ℓ), $\ell = 1, 2$, the semi-axes of the ellipses a_ℓ and b_ℓ, $\ell = 1, 2$, the angles φ_ℓ, $\ell = 1, 2$, and the five dilation/contraction coefficients $\delta_1, \delta_2^{(\ell)}, \delta_3^{(\ell)}, \ell = 1, 2$, yielding a total of $M + 2(N_1 + N_2) + 15$ unknowns. We thus require $M \geq 15$.

We next define the collocation points $(\boldsymbol{x}_\ell)_{\ell=\overline{1,M+N_1+N_2}}$, where $\boldsymbol{x}_\ell = (x_\ell, y_\ell)$, the sources $(\boldsymbol{\xi}_k)_{k=\overline{1,M+N_1+N_2}}$, where $\boldsymbol{\xi}_k = (\xi_k^x, \xi_k^y)$, and the sources $\left(\boldsymbol{\eta}_k^\ell\right)_{k=\overline{1,N_\ell}}$, where $\boldsymbol{\eta}_k^\ell = \left(\eta_k^{\ell\,x}, \eta_k^{\ell\,y}\right)$ $\ell = 1, 2$. As in Section 3, we shall assume that the (known) fixed exterior boundary $\partial\Omega$ is a circle of radius R and the outer boundary collocation and source points are chosen as in (3.4) and (3.5).

We choose the inner boundary collocation and source points as

$$x_{M+n} = X_1 + r_1(\vartheta_n)\cos\vartheta_n,\ y_{M+n} = Y_1 + r_1(\vartheta_n)\sin\vartheta_n,\ \vartheta_n = \frac{2\pi(n-1)}{N_1},\ n = \overline{1, N_1}, \tag{6.4}$$

$$x_{M+N_1+n} = X_2 + r_2(\vartheta_n)\cos\vartheta_n,\ y_{M+N_1+n} = Y_2 + r_2(\vartheta_n)\sin\vartheta_n,\ \vartheta_n = \frac{2\pi(n-1)}{N_2},\ n = \overline{1, N_2}, \tag{6.5}$$

$$\xi_{M+n}^x = X_1 + \delta_2^{(1)}\, r_1(\vartheta_n)\cos\vartheta_n,\ \xi_{M+n}^y = Y_1 + \delta_2^{(1)}\, r_1(\vartheta_n)\sin\vartheta_n,\ \vartheta_n = \frac{2\pi(n-1)}{N_1},\ n = \overline{1, N_1}, \tag{6.6}$$

$$\xi_{M+N_1+n}^x = X_2 + \delta_2^{(2)} r_2(\vartheta_n)\cos\vartheta_n,\ \xi_{M+N_1+n}^y = Y_2 + \delta_2^{(2)} r_2(\vartheta_n)\sin\vartheta_n,\ \vartheta_n = \frac{2\pi(n-1)}{N_2},\ n = \overline{1, N_2}, \tag{6.7}$$

and

$$\eta_n^{1\,x} = X_1 + \delta_3^{(1)}\, r_1(\vartheta_n)\cos\vartheta_n,\ \eta_n^{1\,y} = Y_1 + \delta_3^{(1)}\, r_1(\vartheta_n)\sin\vartheta_n,\ \vartheta_n = \frac{2\pi(n-1)}{N_1},\ n = \overline{1, N_1}, \tag{6.8}$$

$$\eta_n^{2\,x} = X_2 + \delta_3^{(2)}\, r_2(\vartheta_n)\cos\vartheta_n,\ \eta_n^{2\,y} = Y_2 + \delta_3^{(2)}\, r_2(\vartheta_n)\sin\vartheta_n,\ \vartheta_n = \frac{2\pi(n-1)}{N_2},\ n = \overline{1, N_2}, \tag{6.9}$$

with the (unknown) parameters $\delta_2^{(\ell)} \in (S^{(\ell_2)}, 1)\, \ell = 1, 2$, (with $0 < S_2^{(\ell)} < 1$ prescribed) and the (unknown) parameters $\delta_3^{(\ell)} \in (1, S_3^{(\ell)})$ with $S_3^{(\ell)} > 1$ prescribed.

The coefficients $(c_k)_{k=\overline{1,M+N_1+N_2}}$ in (6.2), the coefficients $\left(d_k^\ell\right)_{k=\overline{1,N_\ell}}$ $\ell = 1, 2$, in (6.3), the contraction coefficients $\delta_2^{(\ell)}$ and the dilation coefficients $\delta_1, \delta_3^{(\ell)}$ in (3.5), (6.6)-(6.7), (6.8)-(6.9), the coordinates of the centres (X_ℓ, Y_ℓ), the half-lengths of the major and minor axes a_ℓ and b_ℓ and the angle φ_ℓ can be determined by imposing the boundary conditions (2.1c)-(2.1d) and the transmission condition (6.1f)-(6.1i) in a least-squares sense. This leads to the minimization of the functional

$$S(\boldsymbol{c}, \boldsymbol{d}^1, \boldsymbol{d}^2, \boldsymbol{\delta}, \boldsymbol{C}^1, \boldsymbol{C}^2, a_1, b_1, a_2, b_2, \varphi_1, \varphi_2) := \sum_{j=1}^{M} \left[u_1(\boldsymbol{c}, \boldsymbol{\xi}; \boldsymbol{x}_j) - f(\boldsymbol{x}_j)\right]^2$$

$$+\sum_{j=1}^{M}\left[\frac{\partial u_1}{\partial n}(\boldsymbol{c},\boldsymbol{\xi};\boldsymbol{x}_j)-g(\boldsymbol{x}_j)\right]^2+\sum_{j=1}^{N_1}\left[u_1(\boldsymbol{c},\boldsymbol{\xi};\boldsymbol{x}_{M+j})-u_2^{(1)}(\boldsymbol{d}^1,\boldsymbol{\eta}^1;\boldsymbol{x}_{M+j})\right]^2$$
$$+\sum_{j=1}^{N_1}\left[\frac{\partial u_1}{\partial n^-}(\boldsymbol{c},\boldsymbol{\xi};\boldsymbol{x}_{M+j})+\kappa_1\,\frac{\partial u_2^{(1)}}{\partial n^+}(\boldsymbol{d}^1,\boldsymbol{\eta}^1;\boldsymbol{x}_{M+N_1+j})\right]^2$$
$$+\sum_{j=1}^{N_2}\left[u_1(\boldsymbol{c},\boldsymbol{\xi};\boldsymbol{x}_{M+N_1j})-u_2^{(2)}(\boldsymbol{d}^2,\boldsymbol{\eta}^2;\boldsymbol{x}_{M+N_1+j})\right]^2$$
$$+\sum_{j=1}^{N_2}\left[\frac{\partial u_1}{\partial n^-}(\boldsymbol{c},\boldsymbol{\xi};\boldsymbol{x}_{M+N_1+j})+\kappa_2\,\frac{\partial u_2^{(2)}}{\partial n^+}(\boldsymbol{d}^2,\boldsymbol{\eta}^2;\boldsymbol{x}_{M+N_1+j})\right]^2, \tag{6.10}$$

where $\boldsymbol{c}=(c_1,c_2,\ldots,c_{M+N_1+N_2})$, $\boldsymbol{d}^\ell=\left(d_1^\ell,d_2^\ell,\ldots,d_{N_\ell}^\ell\right)$, $\boldsymbol{\delta}=\left(\delta_1,\delta_2^{(1)},\delta_2^{(2)},\delta_3^{(1)},\delta_3^{(2)}\right)$ and $\boldsymbol{C}^\ell = (X_\ell,Y_\ell)$, $\ell=1,2$.

The normal derivatives involved in (6.10) are defined as in Section 4. The minimization of functional (6.10) is again carried out using the MATLAB© optimization toolbox routine `lsqnonlin`.

6.1. **Example 3.** We investigate the retrieval of multiple elliptical inclusions and therefore consider reconstructing two disjoint ellipses of conductivities $\kappa_1 = \kappa_2 = 10$ contained in $\Omega = B(\mathbf{0}, 1)$. The Dirichlet data (6.1d) is given by (5.7) and the Neumann data is generated using the MFS with $M = 200, 100 = N = N_1 + N2 = 50 + 50$, $\delta_1 = 2$ and $\delta_2^{(\ell)} = 0.9, \delta_3^{(\ell)} = 1.1, \ell = 1, 2$, inside and around each of the ellipses (6.1j). An inverse crime is avoided since the inverse solver is applied using $N_1 = N_2 = 48, M = 48$. The initial guesses for the MFS parameters are taken as $\boldsymbol{c}_0 = 0, \boldsymbol{d}_0^1 = \boldsymbol{d}_0^2 = 0, \boldsymbol{\delta}_0 = (1.6, 0.8, 0.8, 1.2, 1.2)$. We considered the following cases:

(a) Ellipses to be reconstructed:

$$\begin{cases} D_1 : & X_1 = -0.3,\, Y_1 = 0,\, a_1 = 0.3,\, b_1 = 0.2,\, \varphi_1 = \pi/6 \\ D_2 : & X_2 = 0.3,\, Y_2 = 0,\, a_2 = 0.3,\, b_2 = 0.2,\, \varphi_2 = \pi/2. \end{cases}$$

Initial guesses: $\boldsymbol{C}_0^1 = (-0.5, -0.1)$, $\boldsymbol{C}_0^2 = (0.5, 0.1)$, $\varphi_0^1 = \pi/5, \varphi_0^2 = 4\pi/7$, $a_{10} = a_{20} = b_{10} = b_{20} = 0.3$.

(b) Ellipses to be reconstructed:

$$\begin{cases} D_1 : & X_1 = 0,\, Y_1 = -0.4,\, a_1 = 0.3,\, b_1 = 0.2,\, \varphi_1 = 3\pi/4 \\ D_2 : & X_2 = 0.3,\, Y_2 = 0.3,\, a_2 = 0.3,\, b_2 = 0.2,\, \varphi_2 = \pi/6. \end{cases}$$

Initial guesses: $\boldsymbol{C}_0^1 = (-0.2, -0.3)$, $\boldsymbol{C}_0^2 = (0.4, 0.4)$, $\varphi_0^1 = 3\pi/5, \varphi_0^2 = \pi/5$, $a_{10} = a_{20} = b_{10} = b_{20} = 0.3$.

(c) Ellipses to be reconstructed:

$$\begin{cases} D_1 : & X_1 = -0.3,\, Y_1 = -0.3,\, a_1 = 0.3,\, b_1 = 0.15,\, \varphi_1 = \pi/3 \\ D_2 : & X_2 = 0.3,\, Y_2 = 0.3,\, a_2 = 0.3,\, b_2 = 0.15,\, \varphi_2 = \pi/6. \end{cases}$$

Initial guesses: $\boldsymbol{C}_0^1 = (-0.2, -0.2)$, $\boldsymbol{C}_0^2 = (0.2, 0.2)$, $\varphi_0^1 = \pi/4, \varphi_0^2 = \pi/5$, $a_{10} = a_{20} = b_{10} = b_{20} = 0.3$.

(d) Ellipses to be reconstructed:

$$\begin{cases} D_1 : & X_1 = -0.4,\, Y_1 = -0.2,\, a_1 = 0.3,\, b_1 = 0.15,\, \varphi_1 = \pi/3 \\ D_2 : & X_2 = 0.4,\, Y_2 = 0.2,\, a_2 = 0.3,\, b_2 = 0.15,\, \varphi_2 = 5\pi/6. \end{cases}$$

Initial guesses: $\boldsymbol{C}_0^1 = (-0.3, -0.3)$, $\boldsymbol{C}_0^2 = (0.3, 0.3)$, $\varphi_0^1 = \pi/4, \varphi_0^2 = 5\pi/5$, $a_{10} = a_{20} = 0.2, b_{10} = b_{20} = 0.1$.

The inclusion identifications at various iteration numbers, `niter`, for cases (a)-(d) are presented in Figures 5(a)-5(d). For thinner ellipses the reconstruction becomes more difficult.

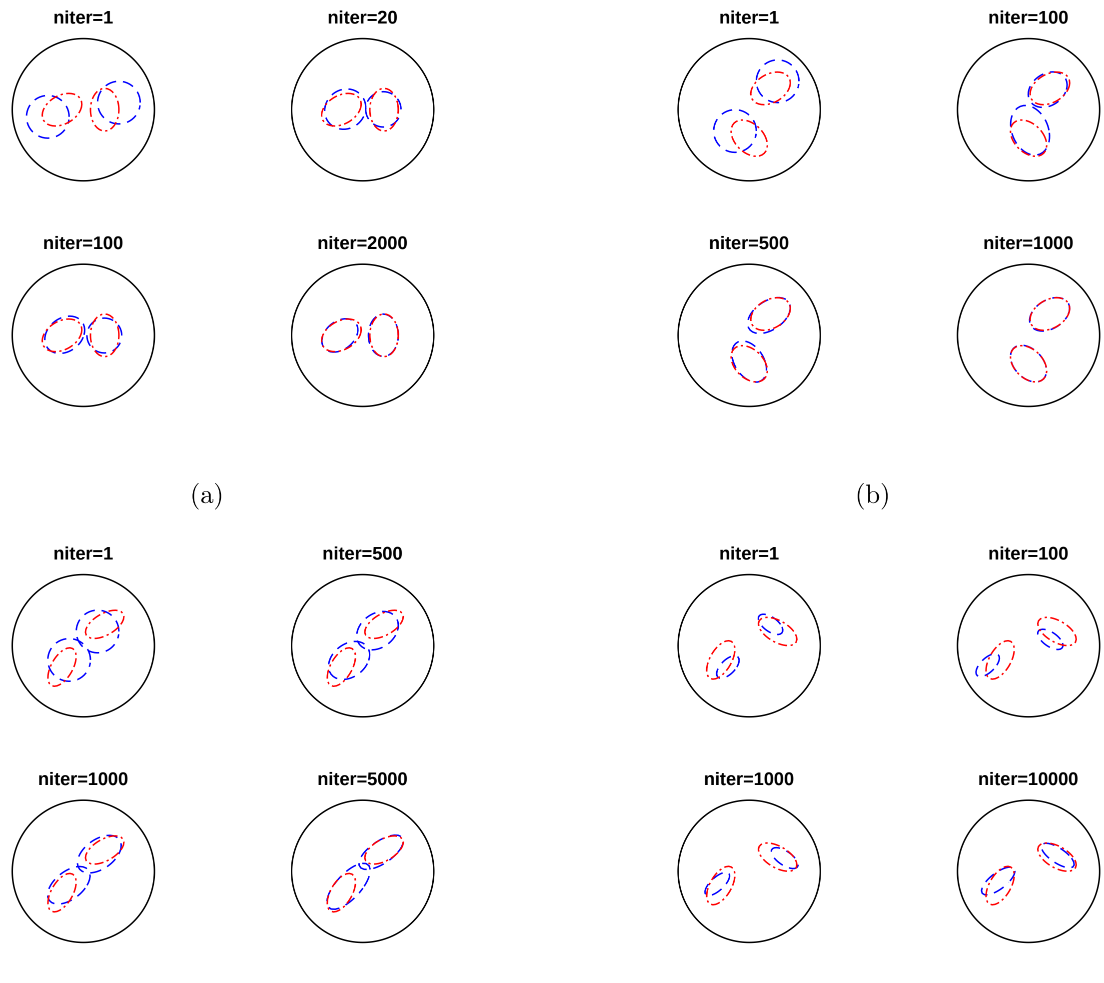

(a) (b) (c) (d)

FIGURE 5. Example 3: Identifications of the elliptical inclusions (a)-(d) at various iteration numbers.

7. Conclusions

We have considered the reconstruction of one (or more) elliptical inclusion(s) in the potential field from a single set of nontrivial Cauchy data using the MFS. The approximation led to a nonlinear minimization problem which was solved using standard software. The results of several numerical experiments revealed that the identification of an ellipse is possible and that the uniqueness result with a single pair of non-trivial Cauchy data seems to hold.

A similar investigation can be carried out in three dimensions examining the unique reconstruction of ellipsoidal inclusions. Furthermore, the uniqueness issue examined in this work can also be investigated for elliptical inclusions in elasticity [20] and acoustics. Finally, anisotropic materials [23] and super-elliptical inclusions [25] could also be the subject of future work. Of course, there is still work to be done theoretically for establishing the uniqueness of an elliptical inclusion and other smooth shapes with one measurement (2.1c)-(2.1d) in the case $0 < \kappa \neq 1 < \infty$ and further insight could perhaps be gained by applying the bifocal Newton algorithm of [28] to analyse uniqueness in nonlinear inverse problems.

Acknowledgements

The authors are grateful to the University of Cyprus for supporting this research.

References

[1] G. Alessandrini and V. Isakov, *Analyticity and uniqueness for the inverse conductivity problem*, Rend. Istit. Mat. Univ. Trieste **28** (1996), 351–369.

[2] K. Astala and L. Paivarinta, *Calderon's inverse conductivity problem in the plane*, Ann. of Math. **163** (2006), 265–299.

[3] H. T. Banks, B. Boudreaux, A. K. Criner, K. Foster, C. Uttal, T. Vogel and W. P. Winfree, *Thermal -based damage detection in porous materials*, Inverse Probl. Sci. Eng. **18** (2010), 835–851.

[4] B. Barceló, E. Fabes and J. K. Seo, *The inverse conductivity problem with one measurement: uniqueness for convex polyhedra*, Proc. Amer. Math. Soc. **122** (1994), 183–189.

[5] M. Dashti-Ardakani and M. Khodadad, *Identification of thermal conductivity and the shape of an inclusion using the boundary element method and the particle swarm optimization algorithm*, Inverse Probl. Sci. Eng. **17** (2009), 855–870.

[6] R. Duraiswami, K. Sarkar and G. L. Chahine, *Efficient 2D and 3D electrical impedance tomography using dual reciprocity boundary element techniques*, Eng. Anal. Bound. Elem. **22** (1998), 13–31.

[7] A. Friedman and V. Isakov, *On the uniqueness in the inverse conductivity with one measurement*, Indiana Univ. Math. J. **38** (1989), 563–579.

[8] V. Isakov, *On uniqueness of recovery of a discontinuous coefficient*, Comm. Pure Appl. Math. **41** (1988), 865–877.

[9] V. Isakov, *Inverse Problems for Partial Differential Equations*, Second edition, Applied Mathematical Sciences, 127, Springer-Verlag, New York, 2006.

[10] O. Ivanyshyn and R. Kress, *Nonlinear integral equations for solving inverse boundary value problems for inclusions and cracks*, J. Integral Equations Appl. **18** (2006), 13–38.

[11] R. L. Johnston and G. Fairweather, *The method of fundamental solutions for problems in potential flow*, Appl. Math. Modelling **8** (1984), 265–270.

[12] H. Kang and J. K. Seo, *The layer potential technique for the inverse conductivity problem*, Inverse Problems **12** (1996), 267–278.

[13] H. Kang and J. K. Seo, *Identification of domains with near-extreme conductivity: global stability and error estimates*, Inverse Problems **15** (1999), 851–867.

[14] H. Kang and J. K. Seo, *Inverse conductivity problem with one measurement: uniqueness of balls in* $\mathbb{R}^3$, SIAM J. Appl. Math. **59** (1999), 1533–1539.

[15] H. Kang, J. K. Seo and D. Sheen, *Numerical identification of discontinuous conductivity coefficients*, Inverse Problems **13** (1997), 113–123.

[16] H. Kang, J. K. Seo and D. Sheen, *The inverse conductivity problem with one measurement: stability and estimation of size*, SIAM J. Math. Anal. **28** (1997), 1389–1405.

[17] A. Karageorghis and D. Lesnic, *The method of fundamental solutions for the inverse conductivity problem*, Inverse Probl. Sci. Eng. **18** (2010), 567–583.

[18] A. Karageorghis, D. Lesnic, and L. Marin, *A survey of applications of the MFS to inverse problems*, Inverse Probl. Sci. Eng. **19** (2011), 309–336.

[19] A. Karageorghis, D. Lesnic, and L. Marin, *A moving pseudo-boundary method of fundamental solutions for void detection*, Numer. Methods Partial Differential Eq. **29** (2013), 935–960.

[20] M. Khodadad and M. Dashti-Ardakani, *Determination of the location, size and mechanical properties of an elastic inclusion using surface measurements*, Inverse Probl. Sci. Eng. **17** (2009), 591–604.

[21] D. Lesnic, *A numerical investigation of the inverse potential conductivity problem in a circular inclusion*, Inverse Probl. Eng. **9** (2001), 1–17.

[22] The MathWorks, Inc., 3 Apple Hill Dr., Natick, MA, *Matlab*.

[23] N. S. Mera and D. Lesnic, *A boundary element method for the numerical inversion of discontinuous anisotropic conductivities*, Eng. Anal. Bound. Elem. **27** (2003), 1–7.

[24] N. S. Mera, L. Elliott and D. B. Ingham, *Detection of subsurface cavities in IR-CAT by a real coded genetic algorithm*, Appl. Soft Comput. **2** (2002), 129–139.

[25] N. S. Mera, L. Elliott and D. B. Ingham, *The detection of super-elliptical inclusions in infrared computerised axial tomography*, in: Advances in Boundary Element Techniques VII, (eds. B. Gatmiri, A. Sellier and M. H. Aliabadi), EC Ltd., UK, pp. 245–246, 2006.

[26] J. K. Seo, *On the uniqueness in the inverse conductivity problem*, J. Fourier Anal. Appl. **2** (1995), 227–235.

[27] F. Triki and C.-H. Tsou, *Inverse inclusion problem: A stable method to determine disks*, HAL Id: hal-01633360, `https://hal.archives-ouvertes.fr/hal-01633360`

[28] E. Winterfors and A. Curtis, *Numerical detection and reduction of non-uniqueness in nonlinear inverse problems*, Inverse Problems **24** (2008), 025016 (14 pp).

Department of Mathematics and Statistics, University of Cyprus/ Πανεπιστημιο Κυπρου, P.O.Box 20537, 1678 Nicosia/Λευκωσια, Cyprus/Κυπρος
E-mail address: `andreask@ucy.ac.cy`

Department of Applied Mathematics, University of Leeds, Leeds LS2 9JT, UK
E-mail address: `amt5ld@maths.leeds.ac.uk`